Published in final edited form as:
Biopolymers. 2008 August ; 89(8): 643–652. doi:10.1002/bip.20993.

A poke in the eye: Inhibiting HIV-1 protease through its flap-recognition pocket

Kelly L. Damm, **Peter M. U. Ung**, **Jerome J. Quintero**, **Jason E. Gestwicki**, and **Heather A. Carlson***
Department of Medicinal Chemistry, University of Michigan, Ann Arbor, MI 48109-1065

Abstract

A novel mechanism of inhibiting HIV-1 protease (HIVp) is presented. Using computational solvent mapping to identify complementary interactions and the Multiple Protein Structure method to incorporate protein flexibility, we generated a receptor-based pharmacophore model of the flexible flap region of the semi-open, apo state of HIVp. Complementary interactions were consistently observed at the base of the flap, only within a cleft with a specific structural role. In the closed, bound state of HIVp, each flap tip docks against the opposite monomer, occupying this cleft. This flap-recognition site is filled by the protein and cannot be identified using traditional approaches based on bound, closed structures. Virtual screening and dynamics simulations show how small molecules can be identified to complement this cleft. Subsequent experimental testing confirms inhibitory activity of this new class of inhibitor. This may be the first new inhibitor class for HIVp since dimerization inhibitors were introduced 17 years ago.

Combination therapy that includes inhibitors of HIV-1 protease (HIVp) are necessary to treat HIV-infected patients [1]. Currently, there are eight peptidic and two non-peptidic drugs on the market that competitively bind in the active site and inhibit HIVp by mimicking substrates and the transition state of peptide cleavage.[2] The discovery of novel inhibitors is still a very active area of research due to the associated toxicity, poor pharmacokinetic properties, and resistance that has developed to the existing drugs.

HIVp is a C_2-symmetric dimer with its active site located at the dimer interface. The central active site is covered by two glycine-rich, anti-parallel β-hairpins, referred to as the “flaps” (residues 43-58). The conformational behavior of the flap region has been extensively studied.[3] The largest populated states are thought to be closed, semi-open, and open. The semi-open conformation is the most prevalent in the apo state, and the closed state is seen when competitive inhibitors are bound in the active site. Two groups have used Langevin Dynamics (LD) simulations to demonstrate the extensive conformational sampling available to the flaps in the apo state.[4,5] Upon introduction of a ligand into the active site of a semi-open conformation, LD simulations have shown that the ligand will induce the flaps to close and replicate key hydrogen bonds seen in bound crystal structures.[6,7]

Here, we present a novel mode of action for HIVp inhibitors: modulating the conformation behavior of HIVp by targeting the flap-recognition site. Upon substrate binding, each flap closes down and positions its flap tip (residues 49-52) in a highly conserved region on the opposite-side monomer, see Fig. 1a. This region can also be called the “eye” from recent

* Corresponding author. Phone: 734-615-6841; FAX: 734-763-2022; carlsonh@umich.edu, Address: 2555 C C Little, 428 Church Street, Ann Arbor, Michigan 48109-1065.

Supporting Information Available. The Supporting Information provides the coordinates and radii for the MPS pharmacophore model of the eye, the 11 identified compounds from screening, and additional analyses of the LD and MD simulations.

HIVp naming convention (based on the backbone of the dimer resembling the face of a bulldog). When the flaps close over the active site, there is a 5-7 Å shift from the apo form and an inward rotation of each monomer. Also, the “handedness” of the orientation of the flap tips reverses upon closing[4-8].

The flap-recognition site may play a role in the opening of HIVp. Substrate proteins can only access the active site through the open conformation [9], although the mechanism allowing such entry is still under investigation [10]. It has been proposed that curling of the flap tips creates a “hydrophobic cluster” that induces flap opening. [11] This curling mechanism creates hydrophobic contacts between the flap tips and the flap-recognition pocket residues on the same monomer; it has been observed in simulations of flap opening by many groups.[6,12,13]

Targeting the eye site has interesting ramifications for both the closed and open states. If the flaps cannot properly close and coordinate the substrate, the catalytic efficiency of HIVp drops.[12,14-16] If the curling of the hydrophobic flap tips into the eye site drives the conformational change into the fully open state [5,11-13,16], then blocking the interaction may interfere with its ability to open and bind its large substrate. If either – or both – mechanisms are possible, an inhibitor bound to this site would alter the conformational equilibrium of the system. It has been suggested that flap dynamics plays a major role in the association and disassociation of substrates [13,17], and modulating the conformational behavior of the flaps may be a potential mechanism for eluding inhibitor resistance. Furthermore, the reduced binding affinity observed for escape mutants of HIVp has been linked to changes in the flexibility of the system.[16,18]

In this study, we show that a small molecule can be stably bound in the flap-recognition pocket and prevent the flaps from assuming the proper closed conformation. Using solvent mapping to identify binding “hotspots”, we generated a receptor-based pharmacophore model of the eye based on an ensemble of conformations from the semi-open, apo state of HIVp. Our use of ensembles of conformational states is called the Multiple Protein Structure (MPS) method, and the goal of the approach is to identify complementary interactions that are well conserved over the ensemble.[19-22] Those essential interactions define a pharmacophore model used in virtual screening to identify molecules with a potential entropic advantage. A modest database of compounds was screened to identify a small set of lead-like molecules that complemented the MPS model. Because inhibition of the site is unprecedented, a representative molecule was chosen for dynamics simulations to examine the stability of the bound complex before investing in experimental testing. Five independent LD simulations were run for 5 ns each (total of 25 ns of simulation time), and a molecular dynamics (MD) simulation was also conducted for 10 ns. The dynamic simulations revealed remarkable insights into the stability of the bound inhibitor and its ability to control the flaps. The inhibitory activity of our compound was subsequently confirmed through experimental testing. This finding is the first new inhibitor class for HIVp since the dimerization inhibitors were introduced 17 years ago.[23,24] No dimerization inhibitors have been tested in the clinic, and all commercial therapies are competitive inhibitors that bind within the central active site. Other potential allosteric sites on HIVp have been proposed,[3,13,25] but no inhibitors have been identified.

Results

The MPS Pharmacophore Model

The eye site is primarily hydrophobic in character, which is fitting given its role in recognizing the hydrophobic residues of a flap tip. The lower portion of the cleft is defined by V32, G78-P81, and I84 while the upper portion is defined by I47-I50, I54, and V56 (Fig.

1b). More distal contacts may be possible with V82 and the backbone atoms of L33, K55, and V77. Six of the twelve residues that define the flap-recognition pocket, G49, V56, G78, P79, T80, and P81, are highly conserved.[26,27] In fact, mutations to the invariant residue T80 are detrimental to enzyme activity, and it is hypothesized that this may be due to altered flexibility of the flap region.[28] The other six residues, V32, I47, G48, I50, I54, and I84, are known to mutate to residues that confer drug resistance to existing protease inhibitors.[26,27] Four of the six common drug-resistant variants, V32I, I47V/A, G48V, and I50V/L, maintain their nonpolar nature in the mutant form. I54 and I84 have been shown to mutate to a variety of residues, although the most common mutations are also hydrophobic, I54V and I84V/A.

An ensemble of semi-open conformations was available from our previous MD simulations of apo HIVp,[20] and these were used to create an MPS pharmacophore model of the eye site, see Fig. 2. The MPS model has seven sites. Three aromatic and two hydrophobic features complement the dominant hydrophobic nature of the cleft. Hydrophobic elements at the bottom of the eye cleft reflect the side chain of I50′, except that the elements show that it might be possible to make slightly deeper interactions within the cleft. A hydrogen-bond donor element complements the backbone carbonyl oxygen of G48, and a hydrogen-bond acceptor complements the backbone amine of I50. The hydrogen-bond acceptor element perfectly reproduces the backbone interaction provided by G51′, the flap tip from the opposite monomer found in the eye site of bound crystal structures.

The MPS model was screened against a modest set of ~34k compounds using MOE. Requiring six of seven pharmacophore elements to be matched, 11 compounds were identified with a molecular weight of ≤ 300 Daltons. The eye cleft is small, and we chose a small size cutoff to avoid any false leads resulting from large, greasy compounds binding in a traditional fashion to the central active site. Compound **1** (2,2,4-trimethyl-1,2-dihydroquinolin-6-yl benzoate) was chosen as the representative inhibitor for dynamics simulations because it had the fewest rotatable bonds and best complemented the bend of the cleft, see Fig. 2. Furthermore, the features of **1** were the closest match to all seven elements. Though it only matches six of the seven features, the conjugated nature of its bicyclic ring is a close approximation of the two closely spaced aromatic features.

The molecules identified for binding in the eye cleft are significantly smaller than existing inhibitors (the other 10 identified compounds are shown in Supporting Information). The molecular weight range for the protease inhibitors currently on the market is 505-720 Daltons, but **1** has a molecular weight of 293 Daltons. Smaller molecules generally have better pharmacokinetic properties, and these entities could have a significant advantage in clinical use over existing HIVp inhibitors. Furthermore, both potential hydrogen bonds are formed with backbone atoms of the protease which may be advantageous for overcoming potential escape mutants. In fact, the co-crystal structure of darunavir, a recently approved nonpeptidic inhibitor, demonstrated key hydrogen bonds to the backbone of both monomers of HIVp[29,30]; darunavir exhibits exceptional broad-spectrum activity against a large panel of MDR HIV-1 strains.[30] Though the sites of hydrogen bonding in the eye are not the same as those between darunavir and HIVp, it shows that targeting the backbone is a feasible way to counteract resistance mutations.

Langevin Dynamics Simulations of Compound 1 in the “Eye”

Analysis of the LD simulations confirmed the stability of the complex. During four of the five simulations, compound **1** continued to interact in a stable fashion with the residues of the flap-recognition pocket as demonstrated by Fig. 3a. However, **1** was seen to temporarily dissociate and rebind to the eye site. For example, during Run 1 (blue trajectory) at 1.3 ns, compound **1** disassociated from the eye pocket into the solvent but returned to its original binding pose after 500 ps. However, the behavior of **1** during Run 2 (purple trajectory) was

the most intriguing. At 2 ns, compound **1** disassociated from the pocket and into the central active site. Over the following nanosecond, it traversed the active site and associated into the flap-recognition pocket of the opposite side monomer, assuming the initial binding pose in the other eye site, Fig. 3b,c (additional snapshots are provided in Supporting Information)! After ~100ps, **1** flipped 180° and maintained this pose for the duration of the simulation. Docking studies with AutoDock 3 [31] also predicted both binding modes (data not shown); hence, it may be possible for **1** to adopt both poses. Fig. 3b,c shows snapshots of the transition of 2-3 ns in Run 2. Though the handedness of the flaps remains the same, the packing shifts with the translocation of the compound.

The effect of bound compound **1** on the dynamics of the protease was also characterized. The LD simulations were chosen to provide a great deal of conformational variation. Fig. 4a reveals representative conformations sampled over Run 3 (conformations from all five LD simulations are provided in the Supporting Information). It is very encouraging to see that compound **1** can complement the eye site in many conformations. This is likely the result of our MPS models incorporating the behavior of the protein across an ensemble of conformational states and may yield an entropic benefit.

The flaps of the protease widely sampled about the semi-open state during LD (Fig. 4a); to quantify the vertical movement of the flaps, the distance between the flap-tip residue I50 and the catalytic residue D25 was calculated for each monomer. In the 1HHP crystal structure of the apo form, the distance is 17.2 Å. The distance averaged 19 Å varied between 15-25 Å over the simulations (Supporting Information). The monomer with **1** bound was slightly more stable than the opposite monomer (the standard deviation for its I50-D25 distance was 2 Å, as opposed to 3 Å for I50′-D25′). Furthermore, the flap of the opposite, unbound monomer frequently sampled a “collapsed” conformation (I50′-D25′ ≤ 14.1 Å, which is the distance seen in closed conformations). Fig. 3c shows additional asymmetry across the flaps, occurring when the flap tips associate. Over the course of the sampling, contact between the flaps was frequently observed, and correlated dynamics analysis clearly showed frequent, ordered motion between the flap tips (Fig. 4b,c). The transient organization between the flap tips was intriguing, especially given the large flexibility seen in the simulations. We turned to explicit-solvent MD simulations to more accurately model the system. The use of explicit water allows for a more accurate representation of solvation and its ability to drive hydrophobic association.

Molecular Dynamics Simulations of Compound 1 in the “Eye”

Compound **1** remained bound in the flap-recognition pocket in a stable fashion. At the beginning of the simulation, it disassociated into the solvent but, after only 250 ps, returned to the eye pocket in its initial binding pose. After this, a consistent binding pose was maintained; the RMSD was 1.7 ± 0.5 Å (the average position of **1** over the MD simulation was used as a reference state). The 1,2-dihydroquinoline core remained in a stable position while the benzoate moiety flipped throughout the simulation.

It was surprising to find that the explicit water promoted a closed form of HIVp (Fig. 5)! It is important to stress that the system was initiated from a complex with HIVp in the semi-open, apo form. The complex was fixed while the water was equilibrated around it, so the initial setup of the water did not force an inappropriate collapse of the protein.[32] It occurred over the last 300 ps of equilibration where the protein was finally allowed to relax. A smaller degree of continued relaxation can be seen in the RMSD of the system over the first 2 ns (Supporting Information).

How is the protease able to assume a closed conformation with **1** bound in the flap-recognition pocket? Blocking the eye should prevent the flaps from closing. Careful

examination revealed that this is an alternative closed state, not the same state seen in bound crystal structures of HIVp [8]. It is well established that the orientation of the flaps reverses in going from the apo state to the closed form [4-7], but the presence of **1** in the eye prevents the flaps from properly folding down. Instead, they form an alternative closed state that maintains the "handedness" of the apo form (Fig. 5). The flaps do not change orientation, so the tips do not occupy the other monomer's flap-recognition pockets. It is very likely that this state could render HIVp inactive as the substrate will not be properly complemented for cleavage.

The distances between the flap-tip residues I50/I50′ and D25/D25′ at the bottom of the pocket were calculated for each monomer (Supporting Information). As implied in the LD simulations, the monomer with **1** bound remained slightly more open than the ligand-free flap; respectively, the distances averaged 14.5 ± 0.9 Å and 12.8 ± 0.8 Å for the flaps in the MD simulation. To provide a reference, the distances in the bound crystal structure 1PRO are 14.1 Å. It appears that the flap with **1** is "closed" and the opposite flap is even more closed. As seen in Run 2 of the LD simulations, the presence of **1** creates an asymmetry between the flaps. To further characterize the asymmetry, the distance between flap tip residue G51/51′ and the eye pocket residue T80/80′ was calculated (Supporting Information). The average distance for the monomer with **1** bound is 12.4 Å, but it is 10.6 Å for the ligand-free monomer. The "collapse" of the ligand-free monomer promotes the alternative closed form by stabilizing the opposite flap in accommodating the binding of compound **1**. In fact, when a second ligand is introduced into the system (i.e., one compound in the eye pocket of each monomer in the semi-open state), the complex is not stable (data not shown). The stoichiometry of one compound per monomer may not be possible due to lack of space on the ligand-free side.

Experimental Verification of Predicted Compounds

Given the simulation data to support the stability of the complexes and the promotion of an alternative closed state, experimental testing was pursued. Compound **1** was found to be autofluorescent and could not be evaluated in our FRET-based assay [33,34]. As such, a para-methoxy derivative (compound **2**: 2,2,4-trimethyl-1,2-dihydroquinolin-6-yl 4-methoxybenzoate) was chosen for testing. The compound also fits the MPS pharmacophore model, but slightly exceeded the 300 MW cutoff. Compound **2** was shown to inhibit HIVp; the IC_{50} value was determined to be 18 ± 3 μM, shown in Fig. 6. The binding affinity is modest but falls within the range of a lead-like compound, as does the molecular weight. [35-37] Oprea et al. noted that lead-like guidelines, not drug-like profiles, should be followed in initial phases of drug discovery to filter compounds.[36,38] If drug-like rules were employed, the identified lead compounds may be difficult to optimize while remaining in drug-like space.[39]

Discussion

Finding novel mechanisms to inhibit HIVp is very important to overcoming the resistance associated with current inhibitors and improving pharmacokinetic properties. We have shown in this study that the flap-recognition pocket can accommodate small molecules and remain stable across multiple LD trajectories. Furthermore, the inhibition activity of **2**, a simple derivative of our modeled lead compound, was experimentally verified (IC_{50} = 18 μM). These inhibitors are much smaller than existing protease inhibitors and chemically very distinct. They are non-peptidic and do not contain the usual hydrogen-bonding features of traditional inhibitors (ketoamides, alcohols, vinyl sulfones, etc). Hence, there is little likelihood that they are acting as traditional competitive inhibitors within the enzymatic binding site of HIVp. In fact, modeling showed that **1** is not stable within the central pocket; instead, it will migrate to the new site and form an appropriate complex.

Further clarification of the mechanism of inhibition by enzymatic assay is not possible because allosteric regulators that bind to apo states of proteins exhibit kinetics that are the same as competitive inhibitors. If the inhibitor regulates the flaps, it will reduce the binding of competitive inhibitors in a cross-competition assay, and the kinetics would appear the same as two traditional inhibitors competing for the active site. Structural studies are underway to definitively determine the binding of **2** and its mechanism of action.

The presence of a ligand in the flap-recognition pocket appears to alter the conformational behavior of the flap region, which may directly modify the kinetics of the system. We hypothesize two inhibition mechanisms: A) an inhibitor may bind in the flap-recognition pocket and the resulting altered conformation prevents the substrate's access to the active site or B) the substrate may bind concurrently with the inhibitor, but substrate cleavage cannot occur because the flaps cannot close with the eye occupied. Furthermore, if the flap-tip curling hypothesis is correct, the flaps of HIVp may not be able to sample an open conformation when the inhibitor is bound.

There are several reasons why this new site is so attractive. First, crystal structures show flap recognition is essential in forming the closed conformer. As previously mentioned, if the flaps cannot close appropriately, the substrate is not properly positioned for cleavage. Second, half of the residues defining the eye pocket are highly conserved and may be resistant to escape mutation. Those that do mutate maintain the hydrophobic character which appears to drive the association of our inhibitor. Third, this site is much smaller than the central cavity, so it may yield inhibitors with low molecular weight which could have better pharmacokinetic properties than current HIVp drugs. Fourth, if effective, the new entities could be added to formulations of existing inhibitors as a combination therapy. Lastly, enhanced affinity should be accessible. We stress that no optimization has yet been attempted with this inhibitor class.

This study presents a new mode of inhibition of a key therapeutic target. In fact, this may be the first new mechanism of action in ~17 years.[23,24] Targeting the elbow (residues 39-42) and β-sheet region (residues 1-5 and 95-99) have been proposed in the literature as potential inhibition mechanisms,[3] but no actual inhibitors have been identified. The dimerization inhibitors are the only experimentally verified alternative therapies to competitive, active-site inhibitors, but none have made it to the clinic.

Materials and Methods

Multiple Protein Structures Method

Previously,[21] our group conducted independent, 3-ns MD simulations of three unbound structures of HIVp (1HHP[40], 3HVP[41], and 3PHV[42]). MPS from those simulations were used to generate a receptor-based pharmacophore model. Snapshots were taken after equilibration and every 600 ps along each 3-ns MD trajectory; each monomer was considered a separate structure, resulting in a collection of 36 conformations from a total of 9 ns of simulation time. In our aforementioned work[20,21], we focused on mapping the bottom of the central cavity to describe the complementarity of competitive inhibitors. In fact, any features of the solvent mapping that were farther 9 Å from the catalytic acids were ignored; these included probes that occasionally minimized to the eye site.

For this study, the flap – particularly the eye region – was the focus. The base of the flap in each structure was flooded with 500 small molecule probes (benzene, ethane, and methanol). Each structure was then subjected to a multi-unit search for interacting conformers (MUSIC) simulation with the BOSS program[43], using the OPLS force field[44], while the protein was held rigid. This resulted in clusters of small molecule probes at favorable interaction

mimima within the eye site of HIVp. Probes were clustered using an in-house program based on Jarvis-Patrick methodology. If 8 probes appeared in a cluster, it was considered significant and included in the consensus step below. For that step, each cluster was represented by its "parent", the probe with the most favorable interactions with the protein.

"Consensus clusters" were determined by aligning the protein snapshots with the equilibrated 1HHP structure and identifying interactions (positions of parent probes) that were common over ≥ 50% of the MPS. Each consensus cluster was then represented in the pharmacophore model as a spherical element. The center of each element was defined by the average position of the probe molecules (benzene centroid, the midpoint of the carbon-carbon bond for ethane, and the oxygen atom of the methanol probe). The radius was based on the RMSD of those features. Individual benzene clusters were labeled aromatic elements whereas ethane clusters were termed hydrophobic. Methanol clusters were classified as a hydrogen-bond donor or acceptor element, based on their interaction with the protein surface. This procedure resulted in a seven-site pharmacophore model of the eye region; the model coordinates are provided in the Supporting Information. Full details of the MPS method can be found elsewhere.[20,45]

Virtual Screening

The MPS pharmacophore model was screened against a virtual dataset (33,623 molecules) based on a subset of compounds available from the University of Michigan's Center for Chemical Genomics. The dataset was screened using the search option within the Pharmacophore Query Editor of MOE[46]. Multiple conformations of each ligand were pre-generated using the default parameters of OMEGA[47] with the exception of the energy window and RMS threshold set to 14 kcal/mol and 1, respectively; the maximum number of conformations was 300. During the database search, a compound was required to fulfill six of the seven features to count as a hit, and the radii of the elements were set to 1.3×RMSD. This produced small, tractable numbers of compounds that were strictly held to the pharmacophore features. The eye model identified 11 compounds within a 300 Daltons molecular weight filter. The predicted poses were manually viewed to verify complementarity and appropriate overlap with the pharmacophore model. Compound **1** was chosen as a model compound for the theoretical simulations because it best complemented the features of the model as described above. The structures of all 11 identified compounds are provided in the Supporting Information.

Dynamics Simulations

Unrestrained, all-atom MD and LD simulations were conducted with AMBER8[48] and the FF99SB force field[49]. The MD simulation used explicit solvation with TIP3P water[50] while aqueous solvation was implicitly modeled using the Generalized Born approach[51] for the LD simulations. Simulations were initiated from the crystallographic coordinates of the apo monomer of HIVp obtained from the PDB[52] (PDB ID: 1HHP[40]), and the homodimer was generated using C_2 symmetry operations in PyMOL[53]. Hydrogens were added via the tLEaP module. MD and LD simulations were performed using the 1HHP dimer in complex with a single copy of compound **1** in eye site of one monomer. The starting coordinates for **1** were obtained from the binding pose generated in the MOE pharmacophore screen. The Antechamber module with the GAFF[54] force field and AM1-BCC charges[55] was used to determine force field parameters for **1**.

Explicit-solvent, MD simulations were performed for 10 ns using one random-number seed. The hydrogen atoms were first minimized, and then the system was solvated using truncated octahedral boundary conditions with a buffer distance of 12 Å and closeness parameter of 0.5. The +4*e* charge of HIVp was neutralized by the addition of 4 chloride counter ions

placed 10 Å from the protein surface in the most electropositive regions. The simulation was run in the NPT ensemble, and SHAKE was used to constrain all bonds to hydrogen atoms. A 2-fs time step was used, along with a 10-Å cutoff for nonbonded interactions and particle mesh Ewald for long-range electrostatics. For the solvated system, the hydrogen atoms were first minimized, followed by side chains, and lastly all atoms. The system was equilibrated in a series of four stages: a gradual heating of water from 10 to 310 K over 50 ps, followed by water equilibration with protein restrained for 250 ps at 310K, then a full system heating from 10 to 310 K over 50 ps, and finally, full system equilibration with the protein unrestrained at 310K for 250 ps. The production phase was run for 10 ns at 310 K.

Five independent LD simulations of HIVp in complex with **1** were run for 5 ns starting from different random-number seeds. Each simulation was run using a 999 Å cutoff for non-bonded interactions. Default dielectric values were used: interior = 1 and exterior = 78.5. The hydrogen atoms were first minimized, followed by a minimization of all atoms. The system was equilibrated over a series of six steps; the first three equilibration steps were each performed for 10 ps, steps four and five over 50 ps, and the sixth step for 100 ps. During the first two equilibration steps, the system was gradually heated from 100 K to 300 K and remained at 300 K for the subsequent steps. Restraints were placed on all heavy atoms and gradually removed over the first four equilibration steps using force constants from 2.0 to 0.1 kcal/mol• $Å^2$. Throughout the fifth equilibration step, the backbone atoms remained restrained with a force constant of 0.1 kcal/mol• $Å^2$. In the sixth, and final, phase of equilibration, all force restraints were removed, and the system was run for 100 ps at 300 K. The subsequent production phase was run for 5 ns. A time step of 1 fs and 1 ps^{-1} collision frequency were used, and SHAKE was employed to constraint hydrogens. This protocol is based on that used by Simmerling and coworkers for HIVp.[4,7]

The correlated dynamics were calculated using the ptraj module, augmented with in-house scripts for visualization and parsing subsets of data. Analyses of the flap conformation and ligand position were also performed with ptraj. The MD trajectory was aligned to its average structure across the 10-ns simulation. However, for LD each trajectory was aligned to the fully minimized 1HHP, the last common structure between the simulations. RMSD traces were calculated for **1** versus its initial position within the eye region. The following metrics were used to quantify the movement of the flaps: the distance between flap tips and catalytic acid (I50 to D25 and I50′ to D25′) and the distance between flap tips and eye pocket (G51 to T80 and G51′ to T80′). Cα atoms were used to measure distance between residues.

HIV-1 Protease Inhibition Assay

A FRET-based assay was available, but unfortunately compound **1** was auto-fluorescent and could not be assayed. However, a para-methoxy derivative of **1** (compound **2**) was available to experimentally test the chemical class. The employed assay is based on a previously described procedure for HIVp.[33,34] The substrate used in the assay is an oligopeptide, RE(EDANS)SQNYPIVQK(DABCYL)R, purchased from Molecular Probes (Cat. No. H-2930). Compounds **1** and **2** were purchased from Chembridge. HIVp was purchased from Bachem Biosciences (Product H-9040). Pepstatin A was purchased from USB (lot #110018) and employed as a control.

Fluorimetric assays were performed, in triplicate, in 384 well plates (Corning No. 3676) and read using a SpectraMax M5 from Molecular Devices. The excitation/emission wavelengths of the substrate are 340/490 nm and employed a cutoff filter at 475 nm. PEG-400 was diluted in Buffer A (20mM phosphate, 1 mM DTT, 1 mM EDTA, 20% glycerol and 0.1% CHAPS at pH 5.1), and 1 μL was added to each well (PEG-400 final concentration, 0.1%) to counter HIVp precipitation, increase solubility of compounds, and prevent aggregation as a false positive. Each compound was dissolved in DMSO then diluted in water, and 2 μL was

added to each well to provide a final concentration range of 1-78 μM for the compound and 1.25-1.87% for DMSO. This was followed by 5 μL of the protease diluted in Buffer A (final concentration of 30 nM). After 45 min of incubation at room temperature, 12 μL of substrate (diluted in Buffer A, final concentration 2 μM) was introduced to initiate the assay, and the fluorescence monitored for 5 min. Given that the concentration of the enzyme is much less than the inhibitor, K_i can be approximated as $IC_{50}/(1+[S]/K_M)$. The concentration of substrate, [S], is much less than its Michaelis constant K_M, previously determined to be 103 ± 8 μM.[33] This makes IC_{50} measured under our conditions a good estimate of K_i, assuming the enzyme kinetics are appropriate with this new mode of inhibition (they are appropriate for both competitive and allosteric inhibition).

Supplementary Material

Refer to Web version on PubMed Central for supplementary material.

Acknowledgments

HAC appreciates the support by a Beckman Young Investigator Award and the National Institutes of Health (GM65372). KLD thanks the Pharmacological Sciences Training Program (GM07767), and JJQ thanks the Molecular Biophysics Training Program (GM008270). KLD is also grateful for receiving a Rackham Predoctoral Fellowship and a fellowship from the American Foundation for Pharmaceutical Education. The authors would also like to acknowledge the Chemical Computing Group for generously providing MOE, and the Center for Advanced Computing at the University of Michigan for valuable computational time. PyMOL[53] was used for various visualization purposes and the creation of figures for this paper.

References

1. Babine RE, Bender SL. Chem Rev 1997;97:1359–1472. [PubMed: 11851455]
2. Eder J, Hommel U, Cumin F, Martoglio B, Gerhartz B. Curr Pharm Des 2007;13:271–285. [PubMed: 17313361]
3. Hornak V, Simmerling C. Drug Discov Today 2007;12:132–138. [PubMed: 17275733]
4. Hornak V, Okur A, Rizzo RC, Simmerling C. Proc Natl Acad Sci U S A 2006;103:915–920. [PubMed: 16418268]
5. Toth G, Borics A. J Mol Graph Model 2006;24:465–474. [PubMed: 16188477]
6. Toth G, Borics A. Biochemistry 2006;45:6606–6614. [PubMed: 16716071]
7. Hornak V, Okur A, Rizzo RC, Simmerling C. J Am Chem Soc 2006;128:2812–2813. [PubMed: 16506755]
8. Wlodawer A, Gustchina A. Biochim Biophys Acta 2000;1477:16–34. [PubMed: 10708846]
9. Rick SW, Erickson JW, Burt SK. Proteins 1998;32:7–16. [PubMed: 9672038]
10. Chang CE, Trylska J, Tozzini V, McCammon JA. Chem Biol Drug Des 2007;69:5–13. [PubMed: 17313452]
11. Scott WR, Schiffer CA. Structure 2000;8:1259–1265. [PubMed: 11188690]
12. Piana S, Carloni P, Parrinello M. J Mol Biol 2002;319:567–583. [PubMed: 12051929]
13. Perryman AL, Lin JH, McCammon JA. Protein Sci 2004;13:1108–1123. [PubMed: 15044738]
14. Baca M, Kent SB. Proc Natl Acad Sci U S A 1993;90:11638–11642. [PubMed: 8265601]
15. Piana S, Carloni P, Rothlisberger U. Protein Sci 2002;11:2393–2402. [PubMed: 12237461]
16. Seibold SA, Cukier RI. Proteins 2007;69:551–565. [PubMed: 17623840]
17. Katoh E, Louis JM, Yamazaki T, Gronenborn AM, Torchia DA, Ishima R. Protein Sci 2003;12:1376–1385. [PubMed: 12824484]
18. Sinha N, Nussinov R. Proc Natl Acad Sci U S A 2001;98:3139–3144. [PubMed: 11248045]
19. Bowman AL, Lerner MG, Carlson HA. J Am Chem Soc 2007;129:3634–3640. [PubMed: 17335207]
20. Meagher KL, Carlson HA. J Am Chem Soc 2004;126:13276–13281. [PubMed: 15479081]

21. Meagher KL, Lerner MG, Carlson HA. J Med Chem 2006;49:3478–3484. [PubMed: 16759090]
22. Damm KL, Carlson HA. J Am Chem Soc 2007;129:8225–8235. [PubMed: 17555316]
23. Weber IT. J Biol Chem 1990;265:10492–10496. [PubMed: 2162350]
24. Zhang ZY, Poorman RA, Maggiora LL, Heinrikson RL, Kezdy FJ. J Biol Chem 1991;266:15591–15594. [PubMed: 1874717]
25. Perryman AL, Lin JH, McCammon JA. Biopolymers 2006;82:272–284. [PubMed: 16508951]
26. Johnson VA, Brun-Vezinet F, Clotet B, Kuritzkes DR, Pillay D, Schapiro JM, Richman DD. Top HIV Med 2006;14:125–130. [PubMed: 16946457]
27. Shafer RW, Rhee SY, Pillay D, Miller V, Sandstrom P, Schapiro JM, Kuritzkes DR, Bennett D. AIDS 2007;21:215–223. [PubMed: 17197813]
28. Foulkes JE, Prabu-Jeyabalan M, Cooper D, Henderson GJ, Harris J, Swanstrom R, Schiffer CA. J Virol 2006;80:6906–6916. [PubMed: 16809296]
29. Ghosh AK, Ramu Sridhar P, Kumaragurubaran N, Koh Y, Weber IT, Mitsuya H. ChemMedChem 2006;1:939–950. [PubMed: 16927344]
30. Ghosh AK, Sridhar PR, Leshchenko S, Hussain AK, Li J, Kovalevsky AY, Walters DE, Wedekind JE, Grum-Tokars V, Das D, Koh Y, Maeda K, Gatanaga H, Weber IT, Mitsuya H. J Med Chem 2006;49:5252–5261. [PubMed: 16913714]
31. Morris GM, Goodsell DS, Halliday RS, Huey R, Hart WE, Belew RK, Olson AJ. J Comput Chem 1998;19:1639–1662.
32. Meagher KL, Carlson HA. Proteins 2005;58:119–125. [PubMed: 15521062]
33. Matayoshi ED, Wang GT, Krafft GA, Erickson J. Science 1990;247:954–958. [PubMed: 2106161]
34. Toth MV, Marshall GR. Int J Pept Protein Res 1990;36:544–550. [PubMed: 2090647]
35. Hann MM, Leach AR, Harper G. J Chem Inf Comput Sci 2001;41:856–864. [PubMed: 11410068]
36. Oprea TI, Davis AM, Teague SJ, Leeson PD. J Chem Inf Comput Sci 2001;41:1308–1315. [PubMed: 11604031]
37. Scapin G. Curr Pharm Des 2006;12:2087–2097. [PubMed: 16796557]
38. Oprea TI, Allu TK, Fara DC, Rad RF, Ostopovici L, Bologa CG. J Comput Aided Mol Des 2007;21:113–119. [PubMed: 17333482]
39. Hajduk PJ. J Med Chem 2006;49:6972–6976. [PubMed: 17125250]
40. Spinelli S, Liu QZ, Alzari PM, Hirel PH, Poljak RJ. Biochimie 1991;73:1391–1396. [PubMed: 1799632]
41. Wlodawer A, Miller M, Jaskolski M, Sathyanarayana BK, Baldwin E, Weber IT, Selk LM, Clawson L, Schneider J, Kent SB. Science 1989;245:616–621. [PubMed: 2548279]
42. Lapatto R, Blundell T, Hemmings A, Overington J, Wilderspin A, Wood S, Merson JR, Whittle PJ, Danley DE, Geoghegan KF, Hawrylik SJ, Lee SE, Scheld KG, Hobart PM. Nature 1989;342:299–302. [PubMed: 2682266]
43. Jorgensen, WL. BOSS 4.2. Yale University; New Haven, Connecticut: 2000.
44. Jorgensen WL, Maxwell DS, TiradoRives J. J Am Chem Soc 1996;118:11225–11236.
45. Carlson HA, Masukawa KM, Rubins K, Bushman FD, Jorgensen WL, Lins RD, Briggs JM, McCammon JA. J Med Chem 2000;43:2100–2114. [PubMed: 10841789]
46. Molecular Operating Environment. Chemical Computing Group Inc; Montreal, Canada: 2001.
47. Omega, 1.8.1. OpenEye Scientific Software; Santa Fe, New Mexico: 2004.
48. Case, DA.; Darden, TA.; Cheatham, TE., III; Simmerling, CL.; Wang, J.; Duke, RE.; Luo, R.; Merz, KM.; Wang, B.; Pearlman, DA.; Crowley, M.; Brozell, S.; Tsui, V.; Gohlke, H.; Mongan, J.; Hornak, V.; Cui, G.; Beroza, P.; Schafmeister, C.; Caldwell, J.; Ross, W.; Kollman, P. AMBER 8. University of California; San Francisco, CA: 2004.
49. Hornak V, Abel R, Okur A, Strockbine B, Roitberg A, Simmerling C. Proteins 2006;65:712–725. [PubMed: 16981200]
50. Jorgensen WL, Chandrasekhar J, Madura JD, Impey RW, Klein ML. J Chem Phys 1983;79:926–935.
51. Still WC, Tempczyk A, Hawley RC, Hendrickson T. J Am Chem Soc 1990;112:6127–6129.

52. Berman HM, Westbrook J, Feng Z, Gilliland G, Bhat TN, Weissig H, Shindyalov IN, Bourne PE. Nucleic Acids Res 2000;28:235–242. [PubMed: 10592235]

53. DeLano, WL. The PyMOL Molecular Graphics System. DeLano Scientific LLC; San Carlos, California: 2002.

54. Wang J, Wolf RM, Caldwell JW, Kollman PA, Case DA. J Comput Chem 2004;25:1157–1174. [PubMed: 15116359]

55. Jakalian A, Bush BL, Jack DB, Bayly CI. J Comput Chem 2000;21:132–146.

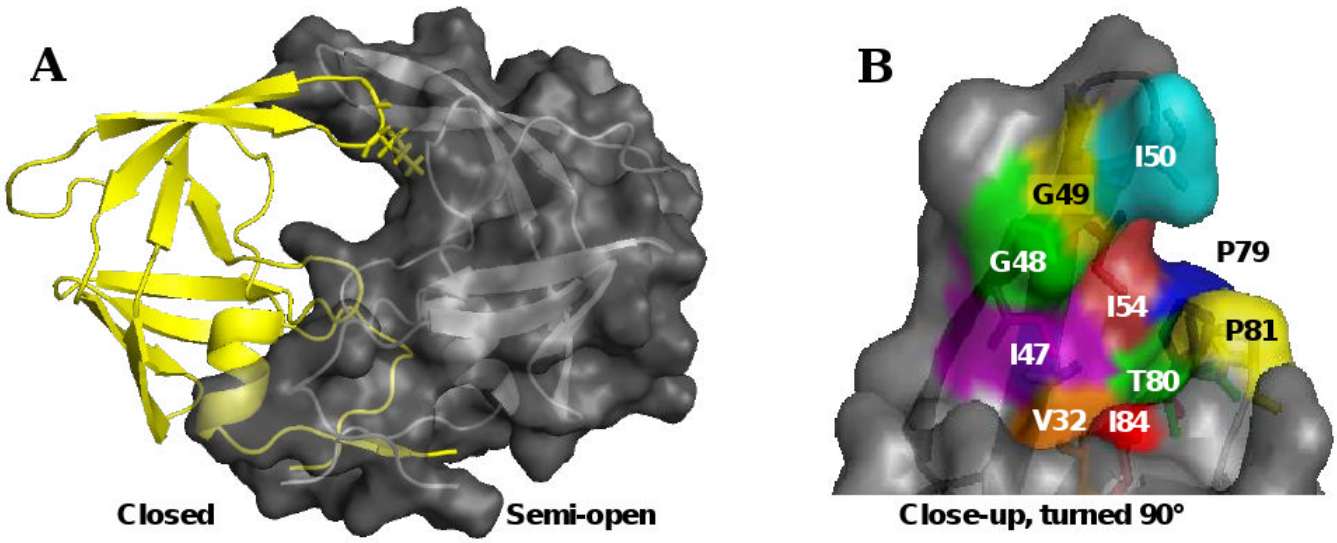

Figure 1.

a) When a monomer closes, it places its flap tips within the flap-recognition site of the other monomer. The right monomer (gray with surface) is the apo, semi-open state that shows the pre-existence of the site. The left monomer (yellow) is in the bound, closed state. I50 and G51 are shown in stick representation in direct contact with the “eye”. **b)** The individual residues within the new eye site are each colored individually and labeled to show their placement within the cleft. G78 and V56 are not visible in this view.

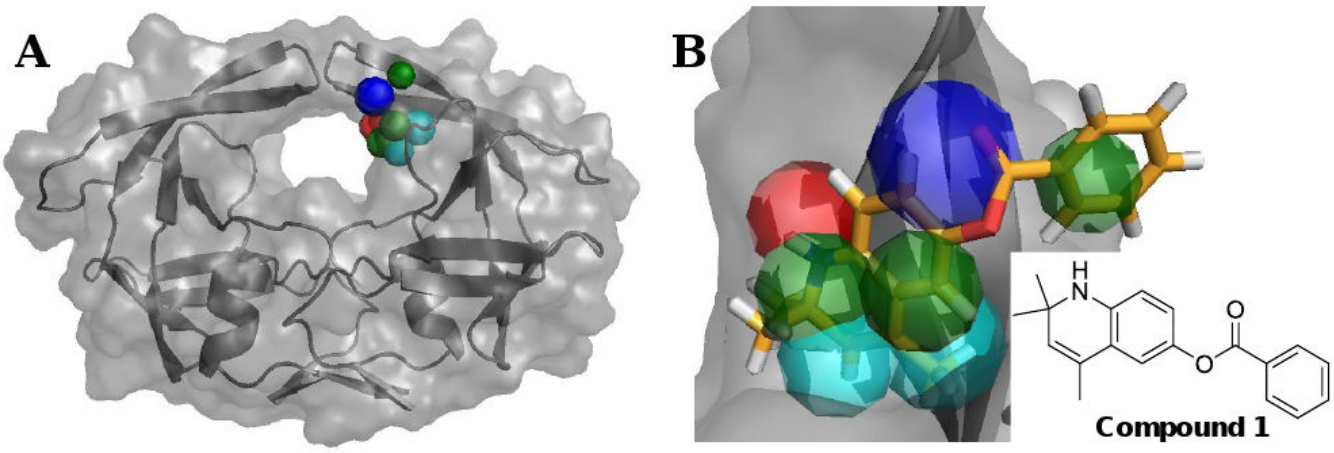

Figure 2.

a) MPS pharmacophore model mapping the eye region of the semi-open conformation. Elements are color-coded according to chemical functionality: red for hydrogen-bond donor, blue for hydrogen-bond acceptor, cyan for hydrophobic, and green for aromatic. **b)** Close-up view of model with a 90° rotation as in Fig 1b. Compound **1** (2,2,4-trimethyl-1,2-dihydroquinolin-6-yl benzoate), identified through the virtual screen, is shown overlaid with MPS pharmacophore model to demonstrate the agreement between its chemical scaffold and the pharmacophore elements.

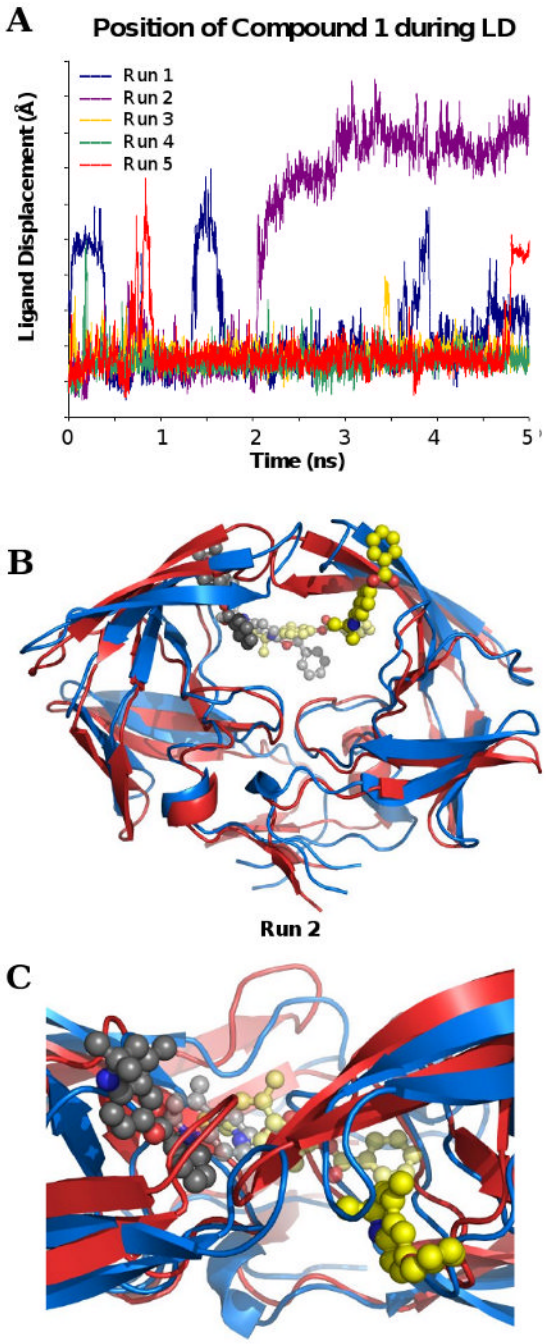

Figure 3.

a) The stability of compound **1** in the eye site is demonstrated by the RMSD to its starting position. Each of the five independent LD is given. Several events are seen where the ligand dissociates and rebinds again in the same pocket (temporary spikes up to 10 Å). In the second simulation (purple line), **1** starts in the flap-recognition pocket of one monomer, disassociates into the central active site, then binds in the eye site of the other monomer. **b)** Representative structures from 2-3 ns of Run 2 show the migration. An early snapshot is shown with a blue backbone and yellow inhibitor; a late structure is shown with a red backbone and gray inhibitor. The transparent inhibitors in the central pocket are actual positions sampled during the migration. **c)** A close-up, top view of the flap region shows

how the flap tips pack against the inhibitor. The handedness stays the same, but the packing shifts from right (blue) to left (red) with the migration of compound **1**.

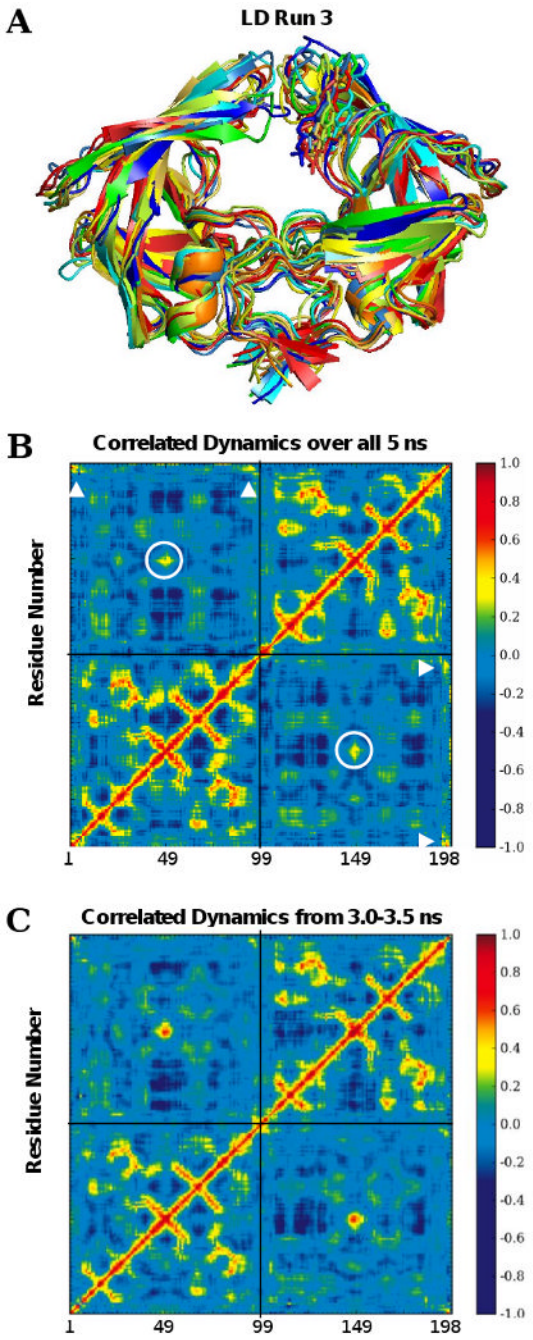

Figure 4.

a) Overlay of snapshots taken every 0.5 ns across the third LD simulation. A large degree of sampling is seen in the flap region. **b)** However, some order is apparent in the correlated dynamics (strong positive correlations are in red and yellow, pronounced anti-correlated motion is dark blue). Over the entire simulation, the strongest positive correlations between the monomers (upper left and lower right regions) are the flap tips (noted white circles) and the C-terminal β-sheets that comprise much of the dimer interface (marked with white triangles). **c)** The strength of the correlation between the flaps varies over the course of the simulation, periodically showing very strong correlations. The periods of strong coupling lasted a maximum of 1.75 ns in Run 1, 1.25 ns in Run 2, and 2.5 ns in Runs 3-5.

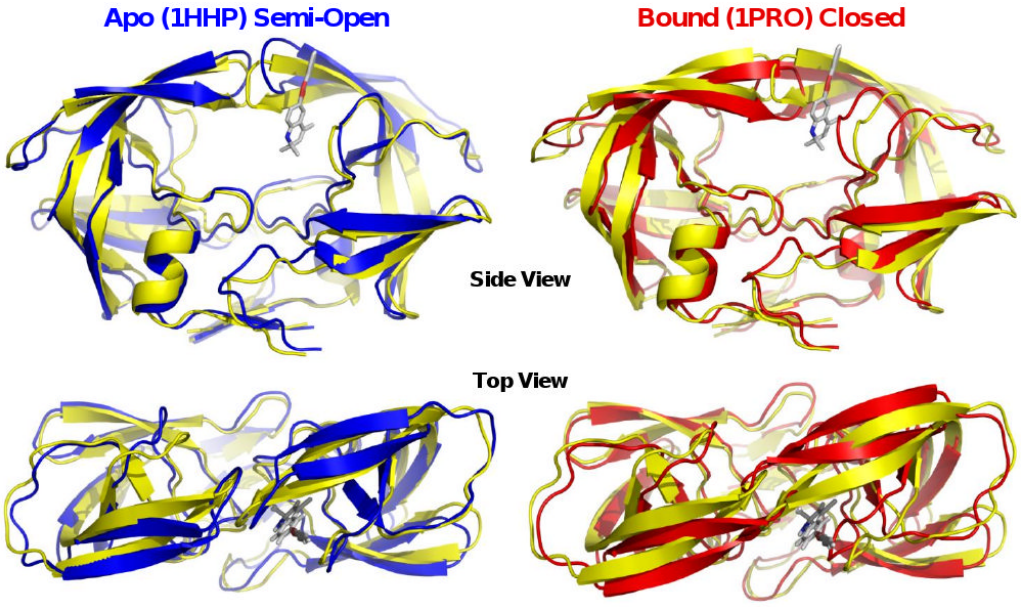

Figure 5.

The average structure from the 10-ns MD simulation is shown in yellow; compound **1** is colored by atom type. The semi-open, apo form is shown in blue, and the closed, bound form is shown in red (co-crystallized inhibitor in the central pocket is not shown for clarity). The MD samples a closed conformation that differs from traditional bound crystal structures. The flaps are lowered, as is appropriate for a closed structure, but the elbows are displaced slightly outward as in the apo state. The handedness of the flaps matches the apo state, not the bound state.

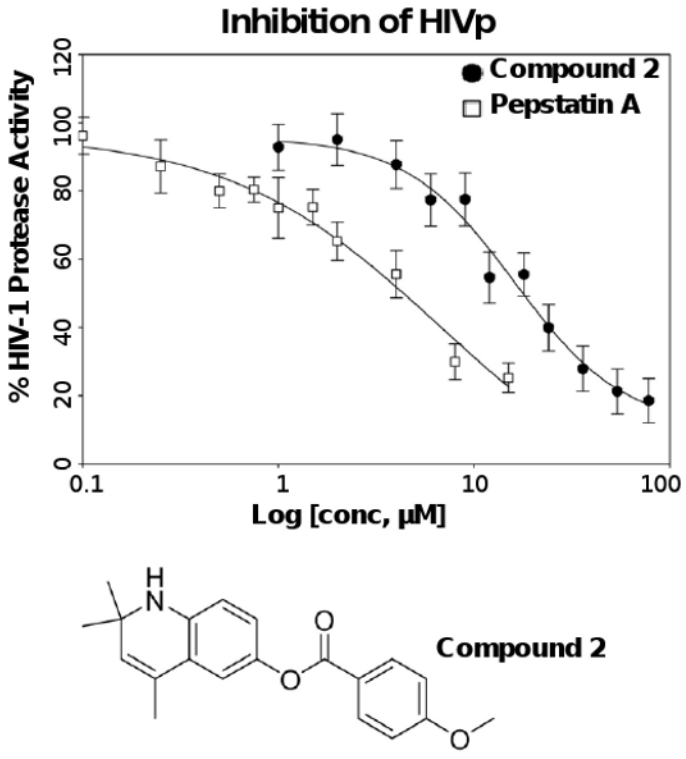

Figure 6.

Compound **2** is a para-methoxy derivative: 2,2,4-trimethyl-1,2-dihydroquinolin-6-yl 4-methoxybenzoate. Its IC_{50} was measured to be 18 ± 3 μM. The activity of HIVp was monitored using a FRET-based assay; upon cleavage of the quenched peptide substrate, fluorescence is recovered. Inhibition is measured as a result of the time-dependent decrease of fluorescence intensity that is linearly related to substrate cleavage. Pepstatin A is shown as a control (IC_{50} = 3.8 ± 0.5 μM under the assay conditions used).